Atmos. Chem. Phys. Discuss., 13, 12771–12796, 2013
www.atmos-chem-phys-discuss.net/13/12771/2013/
doi:10.5194/acpd-13-12771-2013

Atmospheric Chemistry and Physics Discussions

Method development estimating ambient mercury concentration from monitored mercury wet deposition

S. M. Chen[1], X. Qiu[2], L. Zhang[3], F. Yang[2], and P. Blanchard[3]

[1]Department of Mathematics and Statistics, York University, Toronto, Canada
[2]Novus Environmental Inc., Toronto, Canada
[3]Air Quality Research Division, Science and Technology Branch, Environment Canada, Toronto, Canada

Received: 9 April 2013 – Accepted: 30 April 2013 – Published: 14 May 2013

Correspondence to: L. Zhang (leiming.zhang@ec.gc.ca)

Published by Copernicus Publications on behalf of the European Geosciences Union.

Abstract

Speciated atmospheric mercury data have recently been monitored at multiple locations in North America; but the spatial coverage is far less than the long-established mercury wet deposition network. The present study describes a first attempt linking ambient concentration with wet deposition using Beta distribution fitting of a ratio estimate. The mean, median, mode, standard deviation, and skewness of the fitted Beta distribution parameters were generated using data collected in 2009 at 11 monitoring stations. Comparing the normalized histogram and the fitted density function, the empirical and fitted Beta distribution of the ratio shows a close fit. The estimated ambient mercury concentration was further partitioned into reactive gaseous mercury and particulate bound mercury using linear regression model developed by Amos et al. (2012). The method presented here can be used to roughly estimate mercury ambient concentration at locations and/or times where such measurement is not available but where wet deposition is monitored.

1 Introduction

Atmospheric mercury (Hg) is operationally defined as gaseous elemental Hg (GEM), gaseous oxidized Hg (GOM) or reactive gaseous Hg (RGM), and particulate-bound Hg (PBM). Such a practice has been used in field data collections as well as in Hg transport models simulations. Speciated atmospheric Hg data are useful in studies on various topics, e.g., identifying Hg source–receptor relationships (Lynam et al., 2006; Swartzendruber et al., 2006; Choi et al., 2008; Rutter et al., 2009; Weiss-Penzias et al., 2009; Huang et al., 2010; Sprovieri et al., 2010; Cheng et al., 2012, 2013), understanding Hg cycling and partitioning (Engle et al., 2008; Steffen et al., 2008; Amos et al., 2012), evaluating Hg transport models (Baker and Bash, 2012; Zhang et al., 2012a), and quantifying Hg dry deposition budget (Engle et al., 2010; Lombard et al., 2011; Zhang et al., 2012b).

ACPD
13, 12771–12796, 2013

To enhance the estimation of Hg dry deposition on a regional scale in North America, a new monitoring network – the Atmospheric Mercury Network (AMNeT: http://nadp.sws.uiuc.edu/amn/) was established recently in North America within the National Atmospheric Deposition Program (NADP) (Gay et al., 2013). However, the spatial coverage of AMNeT, which has around 20 monitoring sites in USA and Canada, is far less than the long-established NADP Hg wet deposition network – the Mercury Deposition Network (MDN), which has more than 100 monitoring sites. While most Hg transport models could produce reasonable GEM values on various spatial and temporal scales, they frequently failed to capture the magnitudes of GOM and PBM values at both urban and rural locations (Baker and Bash, 2012; Zhang et al., 2012a). Thus, it would be potentially useful if GOM and PBM can be estimated at places where no monitoring data is available, but where wet deposition is monitored. This is based on the fact that wet deposition mainly collect soluble Hg species (i.e. GOM and PBM) and the magnitude of Hg ambient concentrations largely affect the amount of wet deposition. The present study aims to develop a method linking ambient GOM and PBM concentrations with Hg wet deposition for the above-mentioned potential application. Monitored data from AMNet (ambient concentrations) and NADP/MDN Network data (wet deposition) were applied to the study.

2 Relationship between ambient concentration and wet deposition

Mercury wet deposition w measured in a rain gauge follows the balance equation (Amos et al., 2012):

$$w = F_{TP} m + F'_{TP} I \quad (1)$$

$$m = PVc \quad (2)$$

where F_{TP} and F'_{TP} are fractions of mercury from ambient scavenged m and from exogenous source I carried by clouds through long range transport. Both fractions are

ACPD
13, 12771–12796, 2013

functions of the local temperature T and precipitation P as specified in Appendix A. Especially, both fractions are zero when P is zero. Furthermore, the scavenged m is a function of the mercury ambient concentration c, precipitation P and the under cloud air column V. For Eqs. (1) and (2), c is measured at an ambient monitoring station, w is measured at a wet deposition station. However, there is considerable uncertainty regarding the atmospheric redox chemistry of Hg (Hynes et al., 2009), and atmospheric measurement methods are subject to artifacts (Gustin and Jaffe, 2010). Hence the above balance equation serves as a guideline (Appendix A).

Clearly, it is impossible to solve the Eqs. (1) and (2) for c since I and V are unknown. Hence we are interested in a more realistic goal: improving the mean estimate of c by using the wet deposition information w through a statistical method. Several super stations were selected for this study to establish the regression model (where both wet deposition and ambient concentrations are measured at the super stations). In the following sections, we first present the mean estimate of c without wet deposition information. This estimate is also useful in identifying extreme c values. Then we present the mean estimate of c with wet deposition information. A new ratio statistics r with Beta distribution is constructed, which fits the empirical density extremely well. Based on the ratio r, we propose an effective mean estimation with correction method, which adapts to the information w, P and T.

3 Statistical model for dry ambient concentrations

When there is no precipitation, we can model the dry ambient Hg concentration as a normalized random variable c_0, where c_0 has a minimum value zero and a maximum value one. We assume c_0 follows a unimodal beta distribution:

$$c_0 \sim B(\alpha_c, \beta_c), \quad \alpha_c > 1, \quad \beta_c > 1 \tag{3}$$

ACPD
13, 12771–12796, 2013

Depending on different parameters α_c, β_c, this unimodal Beta distribution could skew left or right, and could be flat or steep, hence capable of capturing many different dry ambient concentration distributions.

The sum of weekly ambient GOM and particulate bound mercury PBM concentrations (as of total dry Hg concentrations) from AMNet 2009's 11 dry stations were used to estimate α_c, β_c (MD08, NH06, MD97, NJ30, NJ32, NJ54, NY06, NY20, NY43, OH02, VT99, see site information in Zhang et al., 2012b). By the method-of-moment, we got the following estimates: $\alpha_c = 1.28$, $\beta_c = 72.48$.

The mean, median, mode, and standard deviation of this fitted Beta distribution is given in the Table 1. The normalized histogram and the fitted density function is plotted in the Fig. 1 and the fitted empirical density function is plotted in Fig. 2, which clearly indicated a close fit.

4 Statistical model with wet deposition information

When the precipitation information is available, we define a random variable

$$r := \frac{F_{TP} P^{\frac{1}{3}} c}{w^{\frac{1}{5}}} \sim B(\alpha_r, \beta_r). \quad (4)$$

The definition is motivated by the balance Eq. (1). By dividing both side by w, we get $1 = \frac{F_{TP} PVc}{w} + \frac{F'_{TP} I}{w}$. Both terms on the right hand side are positive, and can be interpreted as the percentage of wet deposition. Since I, V is unknown, we are not able to solve this equation for c. On the other hand, a percentage $\frac{F_{TP} PVc}{w}$ could be statistically modeled as a random variable with Beta distribution. Since V is unknown, we are interested in the random variable $\frac{F_{TP} Pc}{w}$. However, we observe that the total dry concentration c is not linear to the wet deposition w and the precipitation P. Instead, a highly nonlinear relationship appears. Especially, a larger value of wet deposition w typically associates

ACPD
13, 12771–12796, 2013

with a moderate increase of dry concentration. With careful fitting and experimenting, we eventually choose ratio r as $\frac{F_{TP}P^{\frac{1}{3}}c}{w^{\frac{1}{5}}}$, rather than $\frac{F_{TP}Pc}{w}$ as the study object.

Using 2009 data from three super stations: MD08, OH02 and VT99, we fit α_r, β_r and get the mean, median, mode, std, skewness of the fitted Beta distribution (Table 2). Figure 3 compares the normalized histogram and the fitted density function, and Fig. 4 demonstrates empirical and fitted Beta distribution of the ratio r, which shows a very close fit.

To estimate dry ambient concentration with wet deposition and precipitation P, we apply Eq. (4) to

$$c = \frac{\bar{r}w^{\frac{1}{5}}}{F_{TP}P^{\frac{1}{3}}}. \quad (5)$$

Note that the mean value $\bar{r}$ is applied in the formula, although it is dependable to precipitation and wet deposition information. We plot the observed dry ambient concentration data from three super stations and the corresponding estimations in Fig. 5. The plot shows that most points are centered around the identity line $y = x$. However, some points are far away from the identity line, which indicates poor estimate in these cases.

To further analyze errors, we define the error as

$$e = c_{\text{true}} - c_{\text{estimate}} \quad (6)$$

and we make the box-plot and the normality plot of estimate error in Figs. 6 and 7.

Both plots in Figs. 6 and 7 show that the error has nearly zero mean, and is symmetric. The normality plot in Fig. 7 shows that the error distribution has a fat tail than a normal distribution. This suggests that though the estimate error could be close to zero for most cases, reliable estimates could not be easily made for extreme cases.

This phenomenon is not unusual for ratio statistics since a deviation in denominator is amplified. We observed extreme small P values, which is amplified in the formula

ACPD
13, 12771–12796, 2013

(5), and caused extremely large estimate of c. We apply the common remedy for ratio statistics by correcting these extreme estimates. The marginal distribution of c from the previous section provides a reliable mechanism to detect extreme values. When the estimate from (5) is above 95 % quantile or below 5 % quantile, we correct the estimate to these quantiles. The corrected estimate shows better centering tendency towards the identity line $y = x$ as shown in Fig. 8.

To isolate the time series effect, which apparently exists in the dataset, we only use the first day data for a sequential raining event. We observe that wet deposition due to the washout effect is less evident for the following days. However, analyzing the decaying effect quantitatively is nontrivial and is a subject of future study. Hence the result of this section applies only to the first day of a sequence of raining days. Furthermore, the parameter α_r, β_r and the definition of ratio r is not optimized. α_r, β_r are obtained by the method-of-moment in the current study, which could be improved by maximum likelihood method. The definition of ration r is experimental, which could also be optimized by a more advanced nonlinear optimization with constraints model.

5 Optimal partitioning

One can further partition total dry ambient concentration into gas and particle phases as suggested in the study by Amos (Amos et al., 2012). Assuming K is the ratio of

$$K = (\mathrm{PBM}/\mathrm{PM}_{2.5})/\mathrm{GOM} \tag{7}$$

However, mercury monitoring data analysis suggested that PBM may reside across all particular matter size spectrums, but not limited to $\mathrm{PM}_{2.5}$ (Feddersen et al., 2012). To address this concern, we modify the Eq. (7) to (7a)

$$K = (\mathrm{PBM}/\mathrm{PM}_{10})/\mathrm{GOM} \tag{7a}$$

ACPD
13, 12771–12796, 2013

Where,

$$\log_{10}(K^{-1}) = a + \frac{b}{T}, \tag{8}$$

$PM_{2.5}$ and PM_{10} are ambient fine particulate matter with size less than 2.5 and 10 µm, respectively. T is ambient temperature in Kelvin. Parameter (a, b) can be fitted by linear regression. Based on monthly mean mercury data, we used the 2009 seven dry stations dataset (MD97, NJ32, NJ54, NY06, NY20, NY43, OH02) and followed the modified approach of (Amos et al., 2012) with the Eq. (7a), as shown in Table 3. The fitted linear portioning model Eq. (8) is plotted in Fig. 9.

Our fitting aligns with Amos' work well (Amos et al., 2012), where, $a = 10$, $b = -2500$, and $R^2 = 0.49$.

With the optimally fitted a and b and an estimate of total dry mercury concentration c in previous sections, we can estimate the gas and particle partition by solving the following system of equations:

$$\frac{\mathrm{GOM}}{\mathrm{PBM}} = 10^{a+b/T}\,\mathrm{PM}_{2.5} \tag{9}$$

$$\mathrm{GOM} + \mathrm{PBM} = c \tag{10}$$

6 Conclusions

We proposed a new approach to estimate mercury dry ambient concentration by using mercury wet deposition information. Several super stations were selected for this study to establish the regression model. We found that the total dry concentration c is not linear to the wet deposition w and the precipitation P. Instead, a highly nonlinear relationship appears. For example, a higher value of wet deposition w typically associates with a moderate increase of dry concentration. With Beta distribution fitting experiment, and using 2009 data, we fit α_r, β_r and get the mean, median, mode, std, skewness of

ACPD
13, 12771–12796, 2013

the fitted Beta distribution. Compared the normalized histogram and the fitted density function, the empirical and fitted Beta distribution of the ratio r shows a very close fit. Furthermore, we partition the dry mercury concentration into gaseous and particle Hg by using linear regression model developed by Amos et al. (2012).

The fundamental idea presented in this paper can be enhanced by the following three future researches: (i) incorporate the time series study and apply more historical data; (ii) optimally design the ratio statistics r; and (iii) optimally fit α_r, β_r. We found that wet deposition due to below-cloud scavenging effect is less evident for the following days. However, analyzing the decaying effect quantitatively is nontrivial and is a subject of future study of time series data. Hence the result of this study applies only to the first day of a sequence of raining days. Furthermore, the definition of ratio r is a result of careful fitting and numerical testing. But we believe it could be further improved by applying more advanced nonlinear optimization techniques. Similarly, the method-of-moment used in the current study to set the parameter α_r, β_r could also be improved.

Appendix A

Formulation of wet deposition change

$$K^* = K^*_{298} \exp\left(-\frac{\Delta H^\circ_{298}}{R}\left(\frac{1}{T} - \frac{1}{T_0}\right)\right) \tag{A1}$$

$$F = f\frac{K^* L_p RT}{1 + K^* L_p RT} \tag{A2}$$

$$L_p = \frac{P\Delta t}{f\Delta Z} \tag{A3}$$

$$F_{max} = f\left[1 - \exp\left(-k'\frac{P}{f}\Delta t\right)\right] \tag{A4}$$

ACPD
13, 12771–12796, 2013

$$\Delta m = -F\,m + \left(1 - \frac{F}{f}\right) I \tag{A5}$$

$$\Delta m = -F_{\max} m + (1 - F'_{\max}) I, \quad \text{when} \quad F > F_{\max} \tag{A6}$$

Equations (A2)–(A6) follow the Appendix of Amos et al. (2012), where we let $f = 1$, $\Delta t = 1$, $\Delta Z = 1$ since our dataset is a uniformly weekly data with the rain gauge as the grid-box. Consequently, we assume the coefficient $F'_{\max} = \frac{1}{2}$ in Eq. (A6). We note that the change of wet deposit Δw is complementary to the change of soluble gas Δm. The sum of $\Delta w + \Delta m$ equals m_T, which is exogenous. Hence the mass balance equations in use in our model are:

$$\Delta w = F\,m + F\,I \tag{A7}$$

$$\Delta w = F_{\max} m + F'_{\max} I \tag{A8}$$

Since F, $F_{\max}$ and $F'_{\max}$ are functions of Kelvin temperature and precipitation, we let

$$F_{TP} = \begin{cases} F & F \ll F_{\max} \\ F_{\max} & \text{otherwise} \end{cases}, \quad F'_{TP} = \begin{cases} F & F \ll F_{\max} \\ F'_{\max} & \text{otherwise} \end{cases} \tag{A9}$$

Hence the Eqs. (A7) and (A8) are unified into

$$\Delta w = F_{TP} m + F'_{TP} I \tag{A10}$$

Acknowledgements. We appreciate all the people who have contributed to the data collection and quality control for the AMNeT and MDN data sets that are used in the present study.

References

Amos, H. M., Jacob, D. J., Holmes, C. D., Fisher, J. A., Wang, Q., Yantosca, R. M., Corbitt, E. S., Galarneau, E., Rutter, A. P., Gustin, M. S., Steffen, A., Schauer, J. J., Graydon, J. A., Louis, V. L. St., Talbot, R. W., Edgerton, E. S., Zhang, Y., and Sunderland, E. M.:

ACPD
13, 12771–12796, 2013

Gas-particle partitioning of atmospheric Hg(II) and its effect on global mercury deposition, Atmos. Chem. Phys., 12, 591–603, doi:10.5194/acp-12-591-2012, 2012.
Baker, K. R. and Bash, J. O.: Regional scale photochemical model evaluation of total mercury wet deposition and speciated ambient mercury, Atmos. Environ., 49, 151–162, 2012.
Cheng, I., Zhang, L., Blanchard, P., Graydon, J. A., and Louis, V. L. St.: Source-receptor relationships for speciated atmospheric mercury at the remote Experimental Lakes Area, northwestern Ontario, Canada, Atmos. Chem. Phys., 12, 1903–1922, doi:10.5194/acp-12-1903-2012, 2012.
Cheng, I., Zhang, L., Blanchard, P., Dalziel, J., Tordon, R., Huang, J., and Holsen, T. M.: Comparing mercury sources and atmospheric mercury processes at a coastal and inland site, J. Geophys. Res.-Atmos., 118, 2434–2443, doi:10.1002/jgrd.50169, 2013.
Choi, H.-D., Holsen, T. M., and Hopke, P. K.: Atmospheric mercury (Hg) in the Adirondacks: concentrations and sources, Environ. Sci. Technol., 42, 5644–5653, 2008.
Engle, M. A., Tate, M. T., Krabbenhoft, D. P., Kolker, A., Olson, M. L., Edgerton, E. S., DeWild, J. F., and McPherson, A. K.: Characterization and cycling of atmospheric mercury along the central US Gulf Coast, Appl. Geochem., 23, 419–437, doi:10.1016/j.apgeochem.2007.12.024, 2008.
Engle, M. A., Tate, M. T., Krabbenhoft, D. P., Schauer, J. J., Kolker, A., Shanley, J. B., and Bothner, M. H.: Comparison of atmospheric mercury speciation and deposition at nine sites across central and eastern North America, J. Geophys. Res.-Atmos., 115, D18306, doi:10.1029/2010JD014064, 2010.
Feddersen, D. M., Talbot, R., Mao, H., and Sive, B. C.: Size distribution of particulate mercury in marine and coastal atmospheres, Atmos. Chem. Phys., 12, 10899–10909, doi:10.5194/acp-12-10899-2012, 2012.
Gay, D. A., Schmeltz, D., Prestbo, E., Olson, M., Sharac, T., and Tordon, R.: The Atmospheric Mercury Network: measurement and initial examination of an ongoing atmospheric mercury record across North America, Atmos. Chem. Phys. Discuss., 13, 10521–10546, doi:10.5194/acpd-13-10521-2013, 2013.
Gustin, M. S. and Jaffe, D.: Reducing the uncertainty in measurement and understanding of mercury in the atmosphere, Environ. Sci. Technol., 44, 2222–2227, 2010.
Huang, J., Choi, H.-D., Hopke, P. K., and Holsen, T. M.: Ambient mercury sources in Rochester, NY: results from Principle Components Analysis (PCA) of Mercury Monitoring Network data, Environ. Sci. Technol., 44, 8441–8445, 2010.

ACPD
13, 12771–12796, 2013

Hynes, A., Donohoue, D., Goodsite, M., Hedgecock, I., Pirrone, N., and Mason, R.: Our current understanding of major chemical and physical processes affecting mercury dynamics in the atmosphere and at air–water/terrestrial interfaces, in: Mercury Fate and Transport in the Global Atmosphere, edited by: Pirrone, N. and Mason, R. P., chap. 14, Springer, 322–344, 2009.

Levine, S. Z. and Schwartz, S. E.: In-cloud and below-cloud scavenging of nitric acid vapor, Atmos. Environ., 16, 1725–1734, 1982.

Liu, H. Y., Jacob, D. J., Bey, I., and Yantosca, R. M.: Constraints from Pb-210 and Be-7 on wet deposition and transport in a global three-dimensional chemical tracer model driven by assimilated meteorological fields, J. Geophys. Res., 106, 12109–12128, doi:10.1029/2000jd900839, 2001.

Lombard, M. A. S., Bryce, J. G., Mao, H., and Talbot, R.: Mercury deposition in Southern New Hampshire, 2006–2009, Atmos. Chem. Phys., 11, 7657–7668, doi:10.5194/acp-11-7657-2011, 2011.

Lynam, M. M. and Keeler, G. J.: Source–receptor relationships for atmospheric mercury in urban Detroit, Michigan, Atmos. Environ., 40, 3144–3155, 2006.

Rutter, A. P., Snyder, D. C., Stone, E. A., Schauer, J. J., Gonzalez-Abraham, R., Molina, L. T., Márquez, C., Cárdenas, B., and de Foy, B.: In situ measurements of speciated atmospheric mercury and the identification of source regions in the Mexico City Metropolitan Area, Atmos. Chem. Phys., 9, 207–220, doi:10.5194/acp-9-207-2009, 2009.

Sprovieri, F., Hedgecock, I. M., and Pirrone, N.: An investigation of the origins of reactive gaseous mercury in the Mediterranean marine boundary layer, Atmos. Chem. Phys., 10, 3985–3997, doi:10.5194/acp-10-3985-2010, 2010.

Steffen, A., Douglas, T., Amyot, M., Ariya, P., Aspmo, K., Berg, T., Bottenheim, J., Brooks, S., Cobbett, F., Dastoor, A., Dommergue, A., Ebinghaus, R., Ferrari, C., Gardfeldt, K., Goodsite, M. E., Lean, D., Poulain, A. J., Scherz, C., Skov, H., Sommar, J., and Temme, C.: A synthesis of atmospheric mercury depletion event chemistry in the atmosphere and snow, Atmos. Chem. Phys., 8, 1445–1482, doi:10.5194/acp-8-1445-2008, 2008.

Swartzendruber, P. C., Jaffe, D. A., Prestbo, E. M., Weiss-Penzias, P., Selin, N. E., Park, R., Jacob, D. J., Strode, S., and Jaeglé, L.: Observations of reactive gaseous mercury in the free troposphere at the Mount Bachelor Observatory, J. Geophys. Res.-Atmos., 111, D24301, doi:10.1029/2006JD007415, 2006.

ACPD
13, 12771–12796, 2013

Weiss-Penzias, P., Gustin, M. S., and Lyman, S. N.: Observations of speciated atmospheric mercury at three sites in Nevada: evidence for a free tropospheric source of reactive gaseous mercury, J. Geophys. Res.-Atmos., 114, D14302, doi:10.1029/2008JD011607, 2009.

Zhang, L., Blanchard, P., Johnson, D., Dastoor, A., Ryzhkov, A., Lin, C.-J., Vijayaraghavan, K., Gay, D., Holsen, T. M., Huang, J., Graydon, J. A., St. Louis, V. L., Castro, M. S., Miller, E. K., Marsik, F., Lu, J., Poissant, L., Pilote, M., and Zhang, K. M.: Assessment of modeled mercury deposition over the Great Lakes region, Environ. Pollut., 161, 272–283, 2012a.

Zhang, L., Blanchard, P., Gay, D. A., Prestbo, E. M., Risch, M. R., Johnson, D., Narayan, J., Zsolway, R., Holsen, T. M., Miller, E. K., Castro, M. S., Graydon, J. A., Louis, V. L. St., and Dalziel, J.: Estimation of speciated and total mercury dry deposition at monitoring locations in eastern and central North America, Atmos. Chem. Phys., 12, 4327–4340, doi:10.5194/acp-12-4327-2012, 2012b.

ACPD
13, 12771–12796, 2013

Table 1. Fitted Beta distribution of the dry ambient concentration.

mean	median	mode	std	skewness
0.0174	0.0133	0.004	0.0151	1.6848

ACPD
13, 12771–12796, 2013

Table 2. Fitted Beta distribution of the ratio *r*.

mean	median	mode	std	skewness
0.01	0.0079	0.0034	0.0080	1.5833

ACPD
13, 12771–12796, 2013

Table 3. Fitted parameters of partitioning model.

a	b	R^2
9.99	−2529.1	0.43

ACPD
13, 12771–12796, 2013

Table A1. List of nomenclatures.

ΔH°_{298}	enthalpy change of formation for Hg_0, equals −90.83
R	universal gas constant, equals 8.32×10^{-2} atm M^{-1} K^{-1}, see Liu et al. (2001);
K^*	Henry's Law constant (water solution) for mercury, equals 0.142344424, follows (A1), see (8) in Liu et al. (2001);
P	precipitation (cm^3 water cm^{-2} surface s^{-1});
T	Kelvin temperature;
f	areal fraction of the grid box experiencing precipitation, equals 1;
L_p	the time-integrated rain water content in the precipitating fraction of the grid box;
Δt	time step, equals 1;
ΔZ	the grid box thickness (cm), equals 1;
k'	washout rate constant, equals 1 cm^{-1}, see Table 2 of Levine and Schwartz (1982);
I	the cumulative mass of gas scavenged via precipitation from clouds;
Δm	the change in mass of the soluble gas due to washout;
Δw	the change in wet deposition in the rain gauge due to washout;
F_{max}	the maximal value of F based on detailed mass transfer calculation by Levine and Schwartz (1982);
F'_{max}	the re-evaporate and partial shrinkage fraction constant based on Liu et al. (2001).
F_{TP}	fraction of gas scavenged from air as a function of T and P;
F_{TP}	fraction of gas scavenged from exogenous cloud as a function of T and P;
s, t	index of sites and time stamp

ACPD
13, 12771–12796, 2013

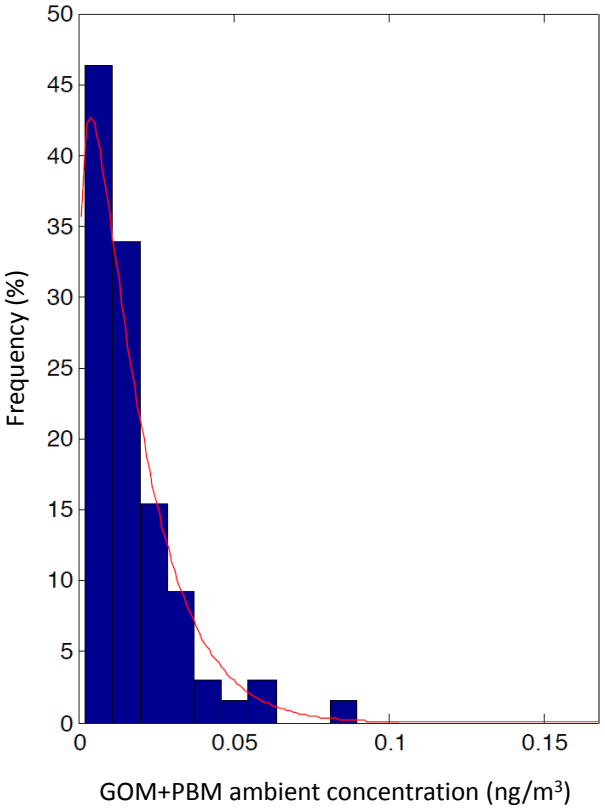

Fig. 1. Normalized histogram (blue bar chart) and fitted Beta distribution (red curve) of the GOM + PBM ambient concentration.

ACPD
13, 12771–12796, 2013

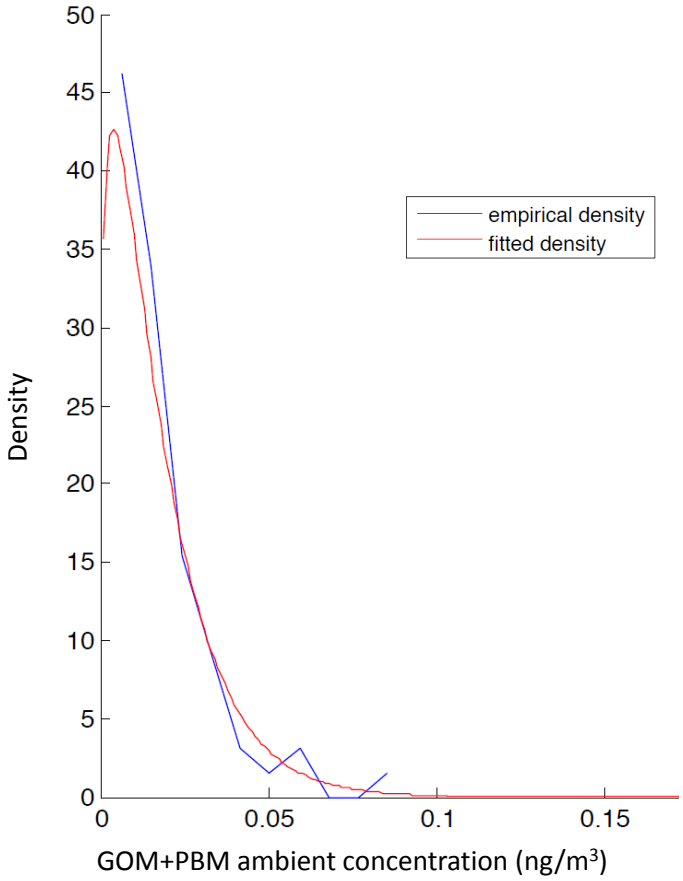

Fig. 2. Empirical and fitted Beta distribution of the GOM + PBM ambient concentration.

ACPD
13, 12771–12796, 2013

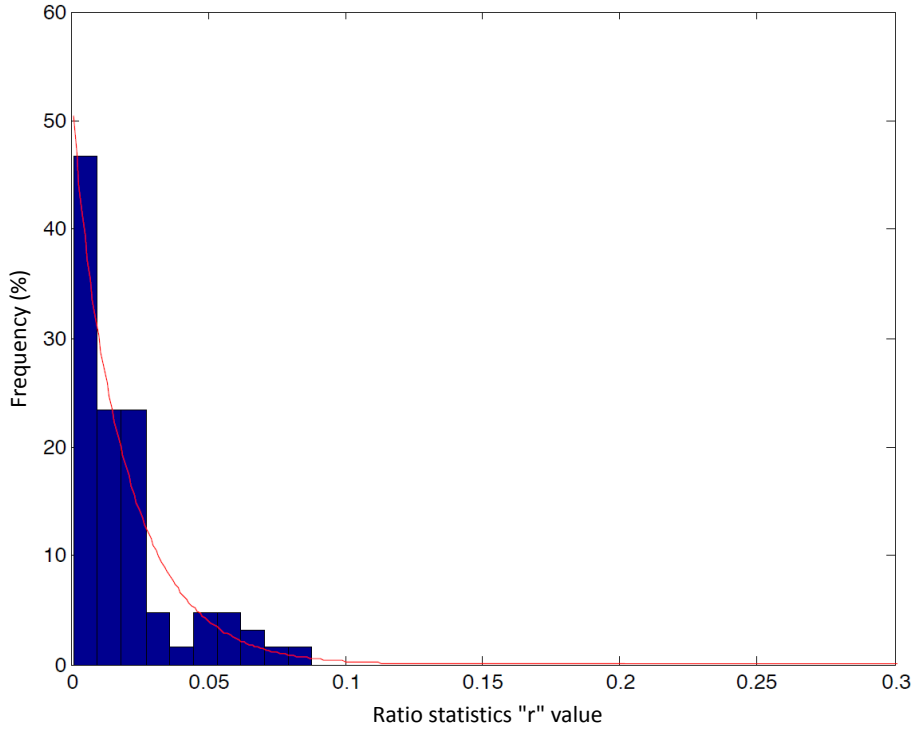

Fig. 3. Normalized histogram and fitted Beta distribution of the ratio *r*.

ACPD
13, 12771–12796, 2013

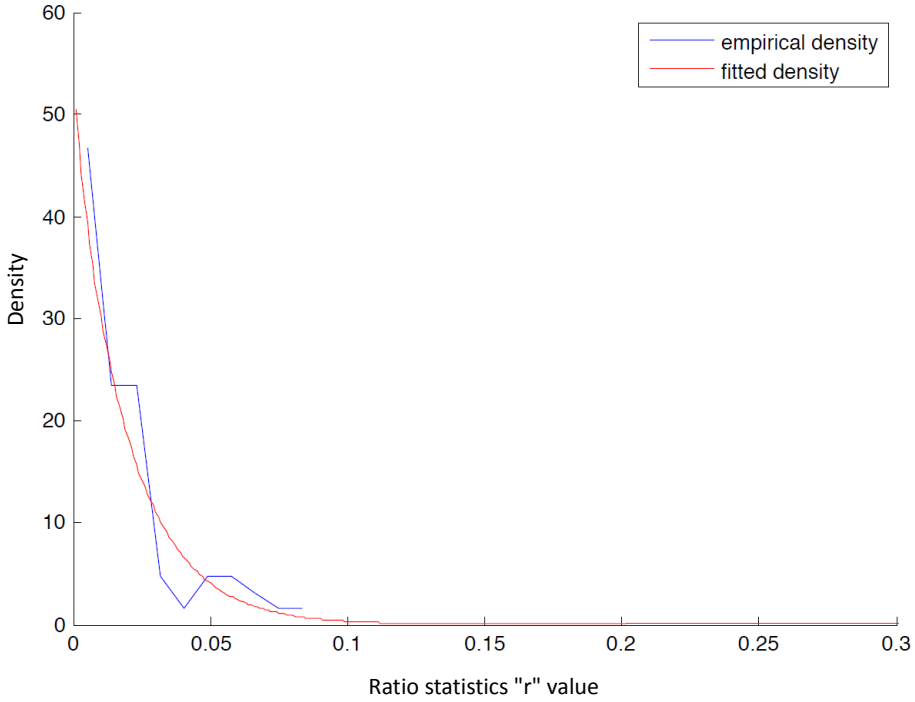

Fig. 4. Empirical and fitted Beta distribution of the ratio *r*.

ACPD
13, 12771–12796, 2013

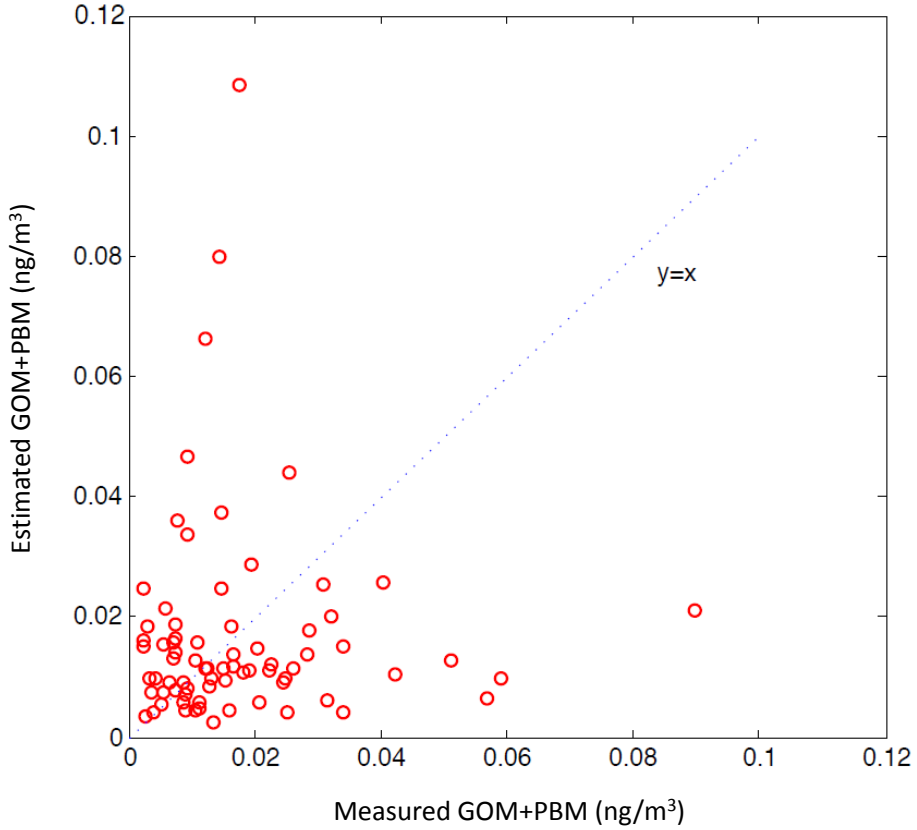

Fig. 5. Estimated versus measured GOM + PBM ambient concentration without correction.

ACPD
13, 12771–12796, 2013

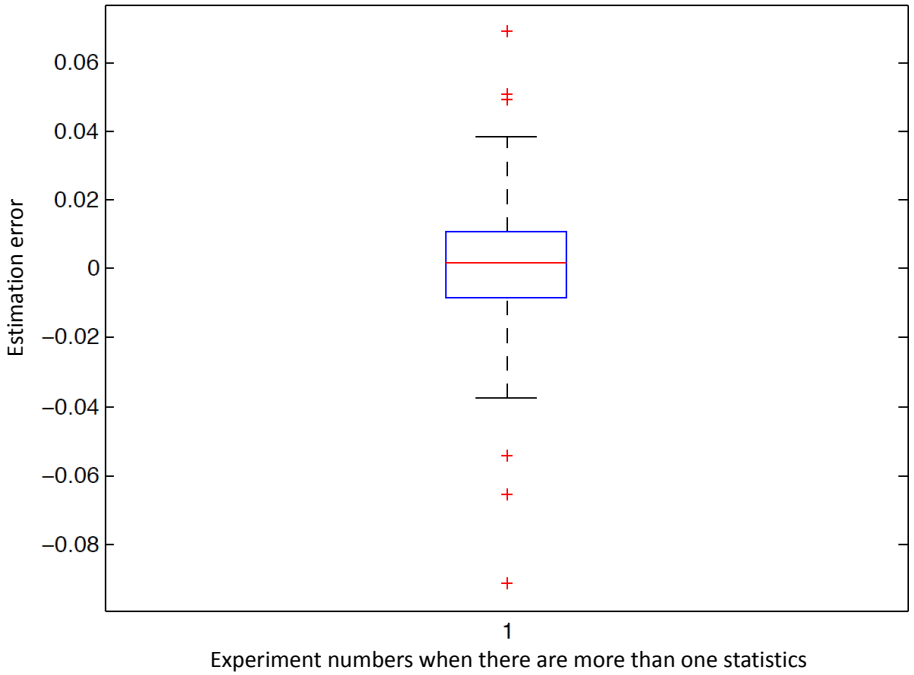

Fig. 6. Boxplot of estimation error.

ACPD
13, 12771–12796, 2013

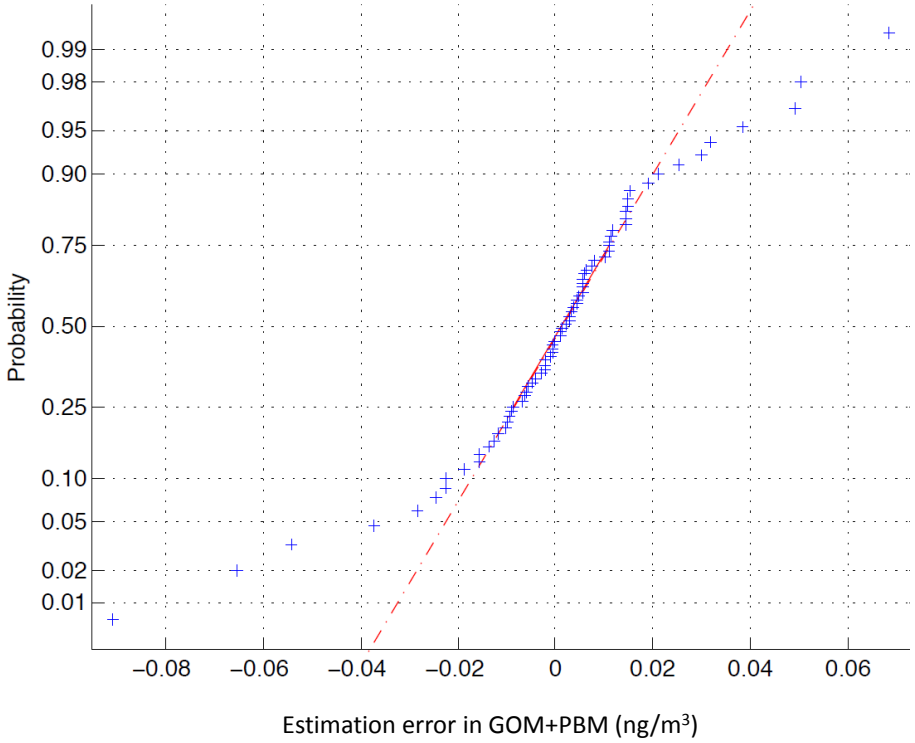

Fig. 7. Estimation error normality plot. A straight line indicates normal distribution.

ACPD
13, 12771–12796, 2013

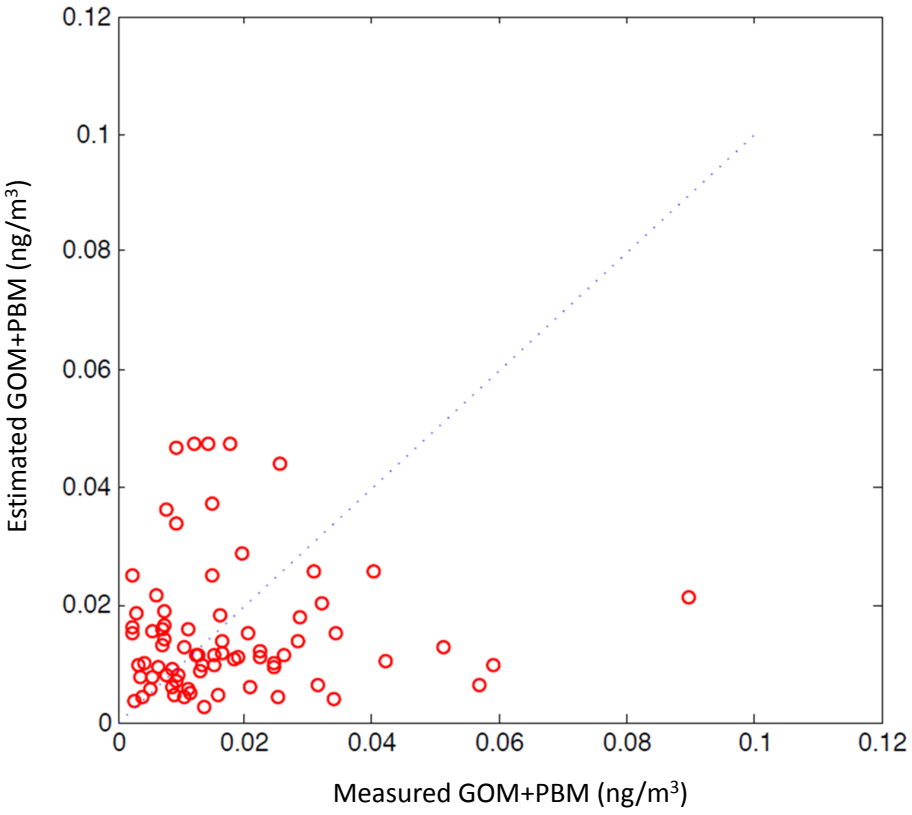

Fig. 8. Estimated versus measured GOM + PBM ambient concentration with correction.

ACPD
13, 12771–12796, 2013

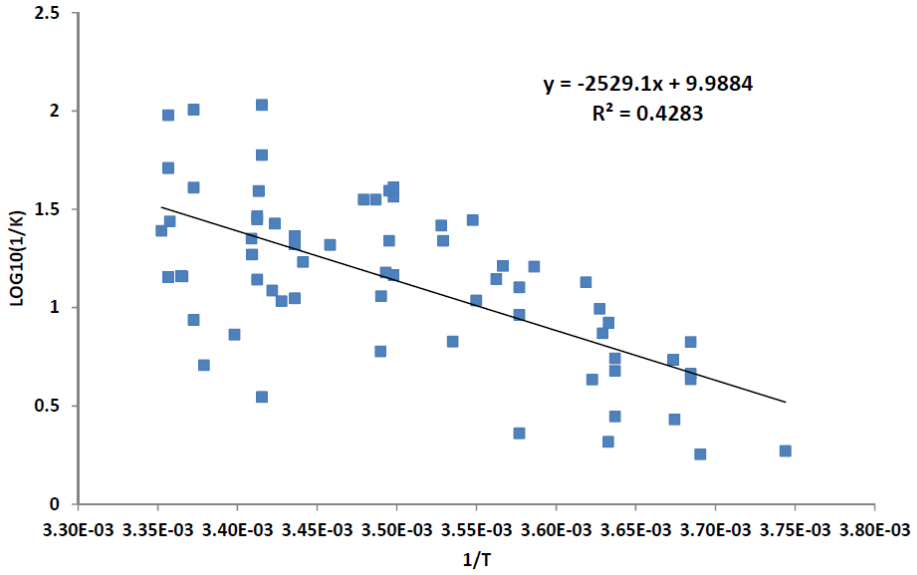

Fig. 9. Fitted linear partitioning model.

ACPD
13, 12771–12796, 2013